Silicon (2024) 16:719–727
https://doi.org/10.1007/s12633-023-02702-1

RESEARCH

Mechanistic Study on the Micro-optical Morphology and Electrical Properties of Microchannel Plates by Acid–Base Alternating Corrosion Processes

Tao Li[1] · Xiaoqing Cong[1] · Jian Wang[1] · Kai Pan[1] · Wankai Li[2] · Ge Jin[1] · Xiangbiao Qiu[1] · Yanjian Lin[1]

Received: 5 July 2023 / Accepted: 30 September 2023 / Published online: 16 October 2023

Abstract
As a two-dimensional vacuum electron multiplier device, the microchannel plate (MCP) is made by solid method with lead silicate glass as the base material, and acid–base etching to remove the core material is a key step in the formation of the microchannel plate, which mainly affects the microstructure, morphology and composition of the inner wall surface, and then affects the electrical properties of the microchannel plate. The microscopic morphology of silicate glass under different etching processes was studied by scanning electron microscopy, and it was found that with the increase of acid–base alternation during the etching process, the particle density of the inner wall of the channel gradually decreased, and the energy spectrum analysis of the particles revealed that the main contents were plumbum (Pb) and bismuth (Bi); further by atomic force microscope (AFM) analysis, the particle peak height was reduced from 31.1 nm to 1.9 nm with roughness. The results of the electrical and noise properties of the microchannel plates show that an appropriate increase in acid–base alternation can effectively reduce the bulk resistance and dark current without reducing the gain of the microchannel plates. This shows that increasing the "erosion intensity" of the acid–base alternation multiple times during corrosion can effectively improve the core-skin diffusion layer, further affecting the physical and chemical transformation of the nanoscale morphology, pointing to a new direction for improving the electrical properties of microchannel plates made of silicate glass.

Keywords Microchannel plate · Nanoscale morphological transformation · Dark current density

1 Introduction

Microchannel plate (MCP) is a high aspect ratio porous lead-silicate glass array structure with electron multiplication properties. With the rapid development of modern science and technology, its application scope has been broadened such as particle detection and micro-optical imaging [1–8], and the demand for detector performance has been increasing, while MCP is facing problems such as high background noise and low gain, which have restricted the further development. Studies of the gain and noise performance of MCP have identified numerous factors affecting noise and gain, among them the reduction of the significant background noise caused by radioisotopes (potassium and rubidium) in photodetector devices by reducing the 40 K content in the glass material [9–12]. One of the most important factors is the inner surface of the micro via, which directly affects the physical processes associated with electron multiplication, and therefore the study of the inner surface of micro via is of great importance to improve gain and reduce background noise. The inner wall surface is formed by the acid and alkaline liquid erosion and hydrogen reduction processes at the core and skin glass diffusion interface, so the different erosion processes directly affect the micro-hole inner wall surface structure and composition. There have been many studies on the surface structure and composition of the inner wall of MCP, mainly focusing on the direct effects of different physicochemical processes on the morphology, structure and composition of the inner wall of MCP, and thus the influence of surface structure morphology and composition on plate volume resistance, electron gain and fixed pattern noise [13–17]. In this paper, the local morphological changes of

✉ Tao Li
447637057@qq.com

[1] North Night Vision Science & Technology (Nanjing) Research Institute Co., Ltd, Nanjing, Jiangsu 211106, China

[2] Institute of Atomic and Molecular Physics, Jilin University, Changchun 130012, China

lead silicate glass on the inner wall surface of MCP channels under the effect of alternating acid and alkali erosion were investigated. At the same time, the electrical properties of MCP were measured under the corresponding conditions, and the relationship between the nanoscale microstructure and the macroscopic electrical properties was established. It is found that acid–base alternation plays a crucial role in the nanoscale morphology and electrical properties.

2 Materials and methods

Leaded silicate glass MCP is manufactured using soluble glass with the raw materials of chemical composition as shown in Table 1. The core glass is hand cast into a glass rod and the skin glass is drawn into a shaped glass tube stretched into fibers, which are then bundled into blocks, sliced and chemically mechanically polished to form a fiber optic plate. The soluble fiber core is chemically etched to form holes, followed by hydrogen reduction and electrode material plating, etc., to make MCP with resistance and emission characteristics.

In this paper, the morphology of the inner wall of the channel is investigated by controlling the number of acid and alkali alternations during the MCP corrosion process, combined with the MCP inner wall roughness and testing, and the noise performance is assessed as a final validation of the process reliability. The acid and alkali etching process is shown in Table 2. The acid concentration was 1 mol/L dilute hydrochloric acid; the base was a NaOH solution with a mass concentration of 5%; and the temperature of the acid–base solution was 25 °C. The corrosion was carried out using a magnetic stirring device to rotate the solution. Between the acid and alkali alternations a pure water ultrasonic cleaning process was used with an ultrasonic frequency of 40 kHz and a power of 300 W. Three sets of acid–base alternating corrosion experiments were performed three times each.

The bulk resistance and gain of the MCP were measured by a vacuum electronic test set-up (VPTF, Nanjing, China), as shown in Fig. 1, with the vacuum of the cavity maintained at better than 1.3×10^{-4} Pa. The body resistance

Table 1 Standard composition of lead silicate glass (%, molar fraction)

	K_2O	Na_2O	BaO	Bi_2O_3	Al_2O_3	SiO_2	PbO
%, Mol Fraction	5.9	1.8	1.1	9	1.4	Bal	20.8

Table 2 Different corrosion processes

Etching Process	Process 1	Process 2	Process 3
Step 1: $Acid^{1st}$		60 min	
Step 2: Lye^{1st}		30 min	
Step 3: $Acid^{2nd}$	60 min	60 min	60 min
Step 4: Lye^{2nd}	60 min	60 min	60 min
Step 5: $Acid^{3rd}$	/	60 min	60 min
Step 6: Lye^{3rd}	/	60 min	60 min
Step 7: $Acid^{4th}$	/	/	60 min
Step 8: Lye^{4th}	/	/	60 min

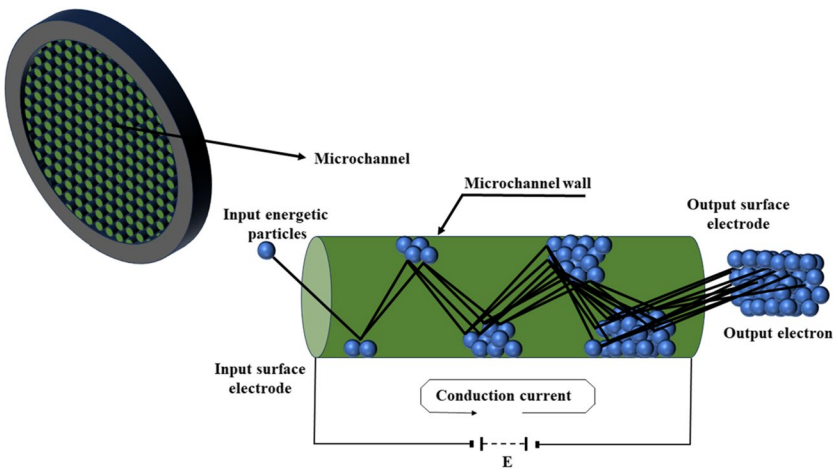

Fig. 1 Schematic diagram of MCP electrical performance and imaging quality testing

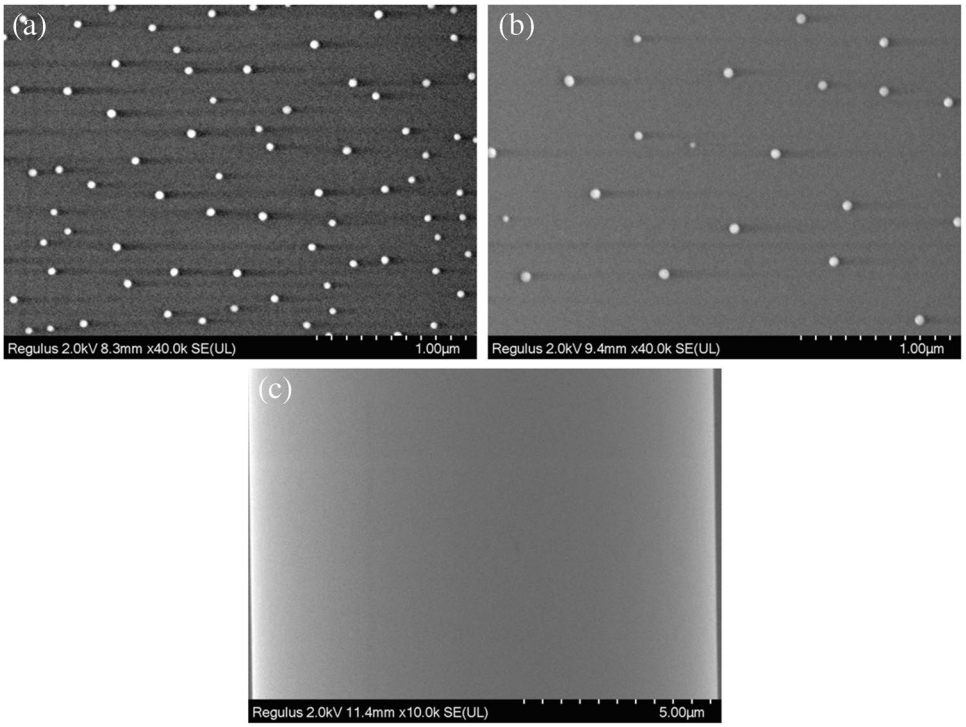

Fig. 2 Shape of the inner wall of the channel with different alternating acid and alkali corrosion processes. **a** Process 1 MCP; **b** Process 2 MCP; **c** Process 3 MCP

of the MCP sample was obtained by measuring the conduction current of the MCP at the corresponding voltage with a microcurrent meter while the MCP input and output were in closed circuit, while the average output current of the MCP was collected from the fluorescent screen and tested with a microcurrent meter. The ratio of the average input current to the average output current is the gain of the MCP. The dark current was also measured at different voltages. The internal surface morphology of the channels was characterized using a swept surface electron microscope (SEM, HITACHI Regulus 8220) and the microscopic morphology of the internal surface of the holes of the MCP was analyzed using an atomic force microscope (AFM, DIMENSION ICON with ScanAsyst) with a contact imaging method. All experimental data were statistically analyzed using SPSS 20.0.

3 Results and Discussion

3.1 The Shape of the Inner Wall of the Channel Under Different Alternating Acid and Alkali Corrosion Processes

The inner wall of the MCP channel will form a reactive surface after acid and alkali etching treatment, which has a greater impact on the subsequent degassing process and the emission performance of secondary electrons, the greater the roughness of the inner wall of the channel, the greater the reactive surface area. Alternating acid and alkali corrosion can effectively reduce the roughness of the inner wall of the channel, while the length of the alkali etching time will have a certain impact on the roughness. It is also considered that after reducing the alkali etching time, the core skin permeation layer may be difficult to remove, and the existence of this permeation layer will not only increase the surface roughness and cause electron memory effect [10], but also increase the adsorption of gas on the inner wall

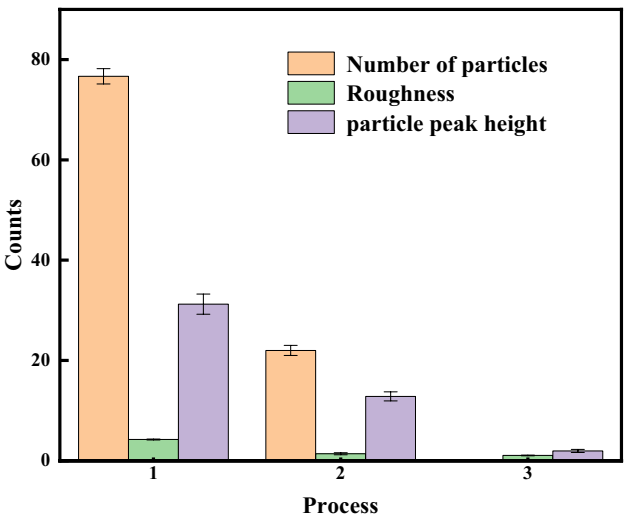

Fig. 3 Variation of MCP roughness, number of internal particles and peak height with different alternating acid and alkali corrosion processes

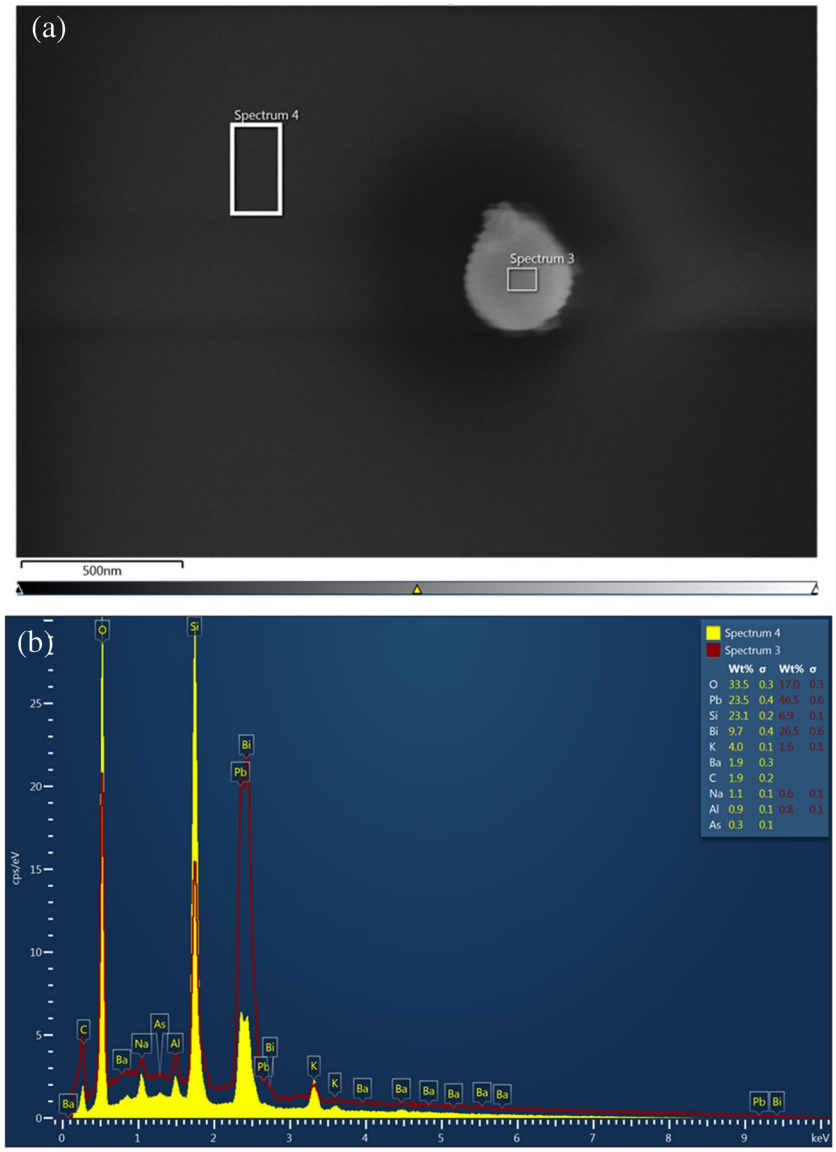

Fig. 4 **a** the inner wall at particle and no particle; **b** EDS diagram

of the channel, which in turn brings ion noise. Therefore, a smooth channel surface is prepared by selecting a suitable etching process. In this paper, we first characterized the inner surface morphology of the channels of MCP treated with the above three corrosion processes using swept surface electron microscopy; secondly, we analyzed the microscopic morphology and roughness of the inner surface of the pores of MCP using atomic force microscopy.

According to Table 2 different acid–base alternating corrosion processes of MCP, after hydrogen reduction and cleaning, test its inner wall surface morphology. From Fig. 2a can be seen, in Process 1 MCP, the channel wall there are more particles; Fig. 2b Process 2 MCP, the channel wall particle number significantly reduced; Fig. 2c Process 3 MCP, the channel wall no obvious particles. Figure 3 shows that with the number of acid and alkali increase the number of particles in the channel wall significantly reduced. It can be speculated that increasing the corrosion intensity of MCP, the core-skin interface diffusion layer changes, and further in the hot hydrogen atmosphere, affecting the reduction of reducible metal oxides in the channel surface aggregation, resulting in changes in the conductive properties and secondary emission characteristics of the channel inner wall surface.

To further determine the particle composition, sample points 3 and 4, the characteristic points of the inner wall of the MCP channel from Process 1, were also selected and their energy dispersive spectrometer (EDS) profiles were measured, as shown in Fig. 4. It is evident from the profiles that the highest content of plumbum (Pb) and bismuth (Bi) in the surface components of the inner wall of the channel may be due to the reduction process producing a new phase, i.e. the aggregation of Pb atoms, resulting in an increase in

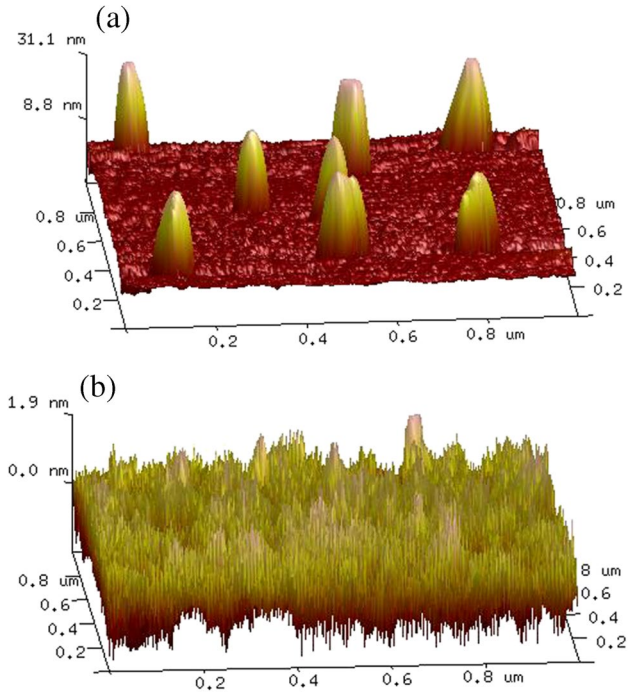

Fig. 5 Microphysical appearance of the inner wall of the channel with different alternating acid and alkali corrosion processes. **a** Process 1 MCP; **b** Process 3 MCP

Table 3 Electrical properties of different acid–base alternating corrosion processes

Sample	Bulk Resistances	Gain	Number
Process 1 MCP	379	15,320	6
Process 2 MCP	216	13,620	7
Process 3 MCP	138	17,213	6

the Z-axis height and surface roughness of the inner wall of the channel. The aggregation of lead atoms is in a diffusely connected state. In the diffusion state, the lead atoms combine into larger lead aggregates and are individually embedded in the bulk glass. After multiple new phases are created, the distance between the lead aggregates becomes smaller and a connected state is formed. At the same time the bismuth atoms produced by reduction also aggregate with the lead aggregates and form new aggregates. Therefore, suitable acid–base alternation during corrosion can improve the surface morphology and elemental distribution of the inner walls of the channels.

Further characterization of the inner wall morphology and roughness testing of the MCP for the three etching processes, Fig. 5a can be seen, Process 1 MCP, the channel inner wall surface appears larger island particles, and island particles peak height 31.1 nm; with the number of acid–base increase the number of island particles and peak height significantly reduced, Process 3 MCP the roughness of 1.9 nm. This acid etching stripping core after the glass skin glass surface appears island structure, these island particles in the fiber drawing have been formed at the interface, indicating that the core skin glass interface diffusion there is mutual reaction diffusion [18].

3.2 Dark Currents and Background Noise Under Different Acid–Base Alternating Processes

This study deals with the comparison and analysis of the electrical properties of microchannel plates (MCP) after being subjected to different acid–base corrosion cycles. Firstly, this article found that the body resistance of MCP showed a decreasing trend with an increasing number of acid and alkaline treatments during the corrosion process. This may be due to changes in the morphology and element distribution of the inner wall of the microchannel caused by the treatment process, resulting in changes in the body resistance after hydrogen reduction. The specific values are given in Table 3.

Furthermore, we also carried out tests on the dark current of MCP and the schematic diagram of the test components is shown in Fig. 6. The results show that the dark current decreases as the number of acid–base treatments increases, and the specific effect is shown in Fig. 7. The reasons for the noise reduction can be summarised as follows: firstly, after alternating acid–alkali etching treatment, the correlation between the inner wall roughness of the microchannel and the surface alkali

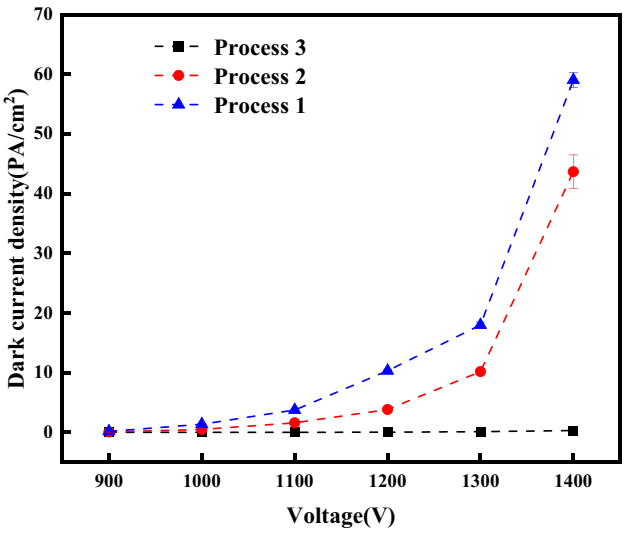

Fig. 7 Variation of dark current density with voltage for different alternating acid and alkali corrosion processes

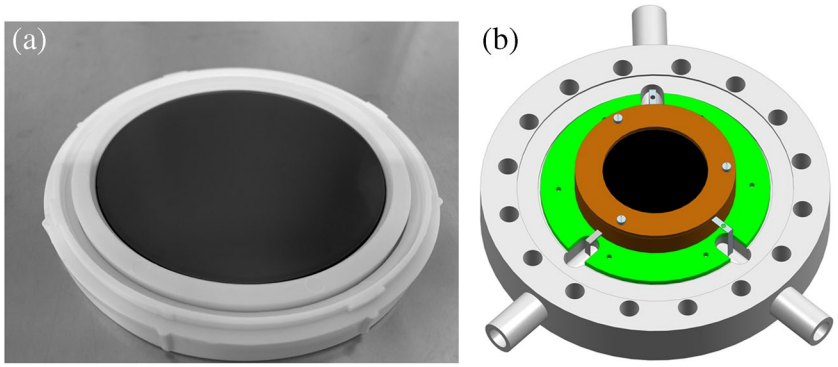

Fig. 6 **a** MCP; **b** Schematic diagram of the Φ88 assembly

metal state is enhanced. Such inner wall roughness is beneficial for the tip discharge, although it may increase the background noise, it is acceptable compared to its beneficial contribution. Secondly, the improvement of the internal wall roughness may encourage more gas to be adsorbed on its surface. Under high operating voltage, these adsorbed gases are likely to be ionized and accelerated in an electric field opposite to the input direction of the channel, resulting in photoelectron collisions. In addition, for alkali metal ions that adhere to the surface of the microchannel, are sensitive to the operating voltage and have a small atomic radius, they may escape from the surface and inner wall of the microchannel and similar ion feedback processes may occur.

To evaluate the accuracy and rationality of the above discussion, we use the background noise measured by the customer's Jilin University laboratory as the evaluation standard. After detailed comparison and analysis, a clear conclusion can be drawn: compared with the process 1 MCP which underwent one stage of corrosion treatment, the process 3 MCP that underwent three stages of alternating acid and alkali etching treatment achieved better noise treatment effects in various parts of the equipment and in the customer's experimental indicators, as shown in Fig. 8.

3.3 Changes in Background Noise Under Different Voltages and Screen Voltages

As the MCP voltage and screen voltage change, the background noise also changes accordingly. We selected the background at a screen voltage of 3800 V and an MCP voltage of 1550 V as the base background subtraction, and measured the trend of background noise changes at fixed screen voltage and different MCP voltage, as well as the trend of background noise changes at constant MCP voltage and different screen voltage, as shown in Figs. 9 and 10. It was found that the number of noise generated with the increase of MCP voltage is much higher than that generated with the increase of screen voltage, as shown in Figs. 11 and 12. This may be due to the low surface potential barrier of MCP material under high voltage, and “hot-spots” caused by debris on the MCP surface are excluded, which make it easy to escape more electrons [19].

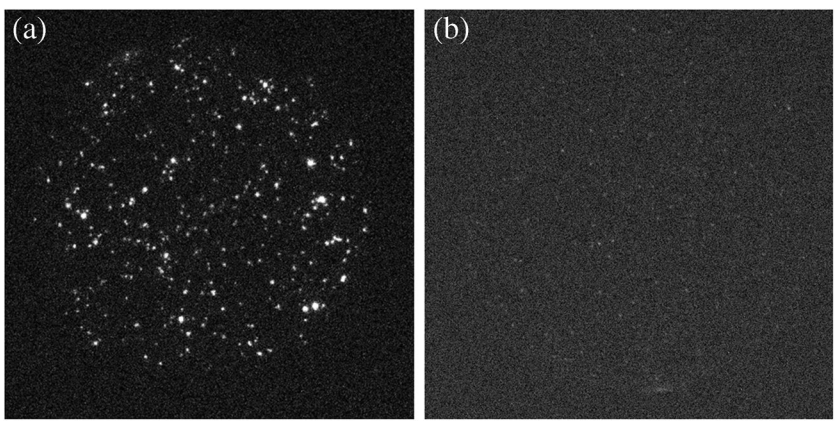

Fig. 8 **a** Background noise for Process 1MCP; **b** Background noise for Process 3 MCP

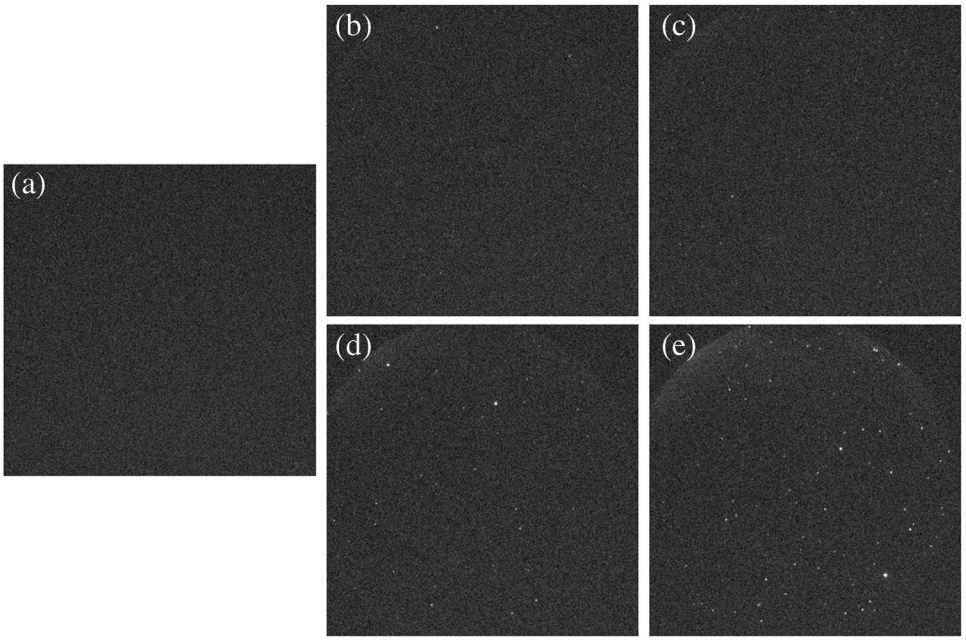

Fig. 9 Screen voltage 3800 V, background noise at different MCP voltages **a** 1550 V; **b** 1700 V; **c** 1750 V; **d** 1800 V; **e** 1850 V

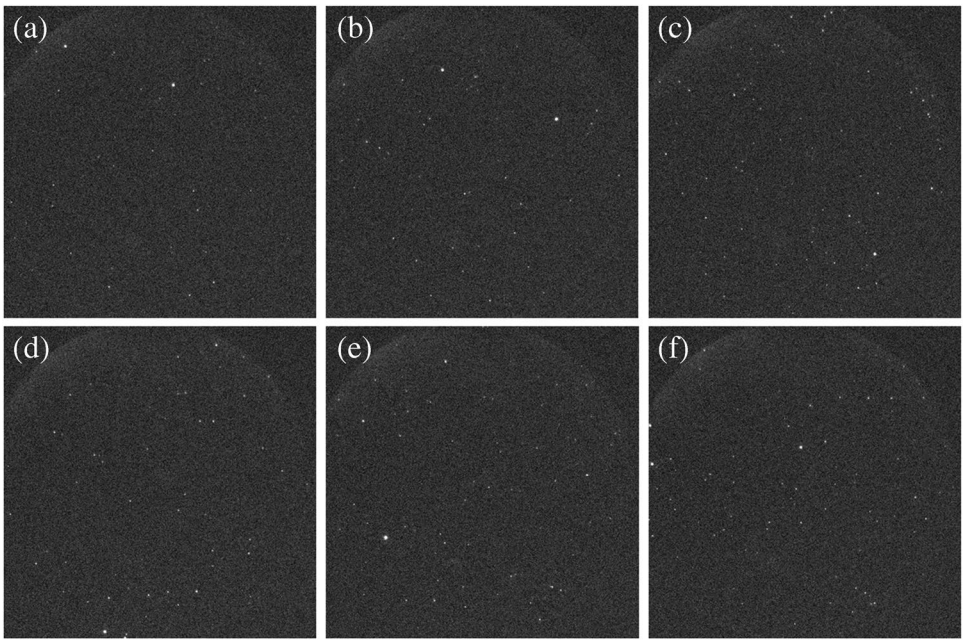

Fig. 10 MCP voltage 1800 V, background noise at different Screen voltages **a** 3800 V; **b** 4000 V; **c** 4200 V; **d** 4300 V; **e** 4400 V; **f** 4500 V

4 Conclusions

The performance of the microchannel plate after different acid–base alternating treatments was investigated according to the mechanism of acid–base corrosion of the microchannel plate. The SEM characterization and AFM roughness test results show that increasing the acid–base alternating corrosion can effectively reduce the formation of inner wall island particles and further reduce the inner wall surface roughness. Performance tests on the dark current of

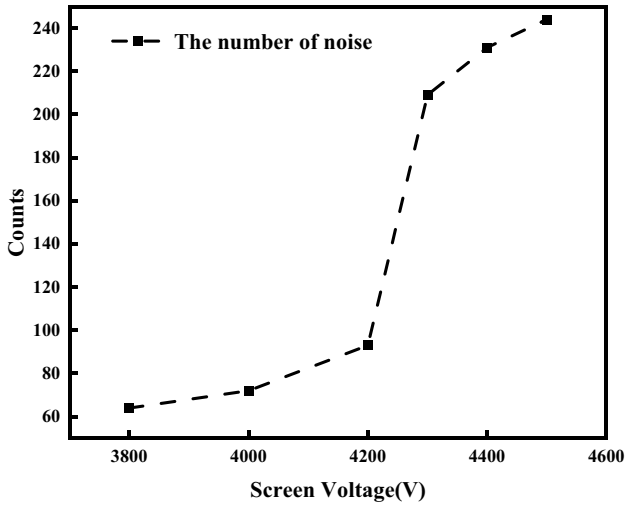

Fig. 11 MCP voltage 1800 V the number of noise changes with the Screen voltage

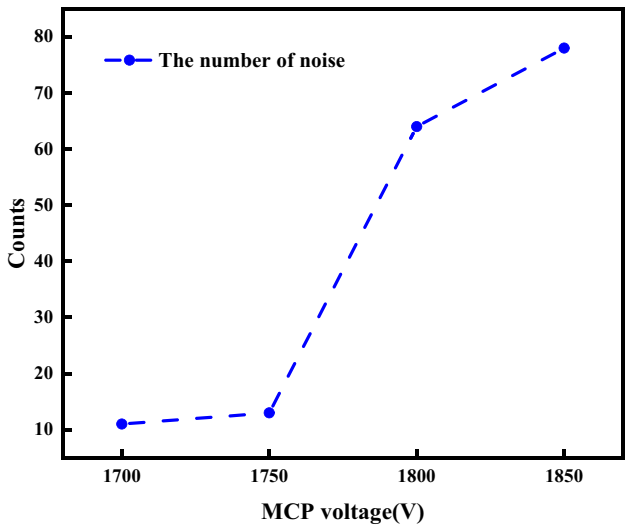

Fig. 12 Screen voltage 3800 V the number of noise changes with the MCP voltage

the microchannel plate reflect that an appropriate increase in acid–base etching can reduce the dark current and reduce the background noise. Therefore, by adjusting the acid–base etching process, it is possible to improve the MCP noise profile without increasing other risk factors.

Acknowledgements The authors express their gratitude to North Night Vision Science & Technology (Nanjing) Research institute Co., Ltd. for financially supporting this study. We also thank Institute of Atomic and Molecular Physics, Jilin University for providing test equipment.

Author Contributions Tao Li: Formal analysis, Data curation, determining the research plan, data analysis, and writing and revised the manuscript. Xiaoqing Cong: Determining the research plan, data analysis. Jian Wang: Determining the research plan, revised the manuscript. Kai Pan: Formal analysis, Data curation, data analysis. Wankai Li: Formal analysis, Data curation, data analysis. Ge Jin: Formal analysis, Data curation. Xiangbiao Qiu: Formal analysis, Data curation. Yanjian Lin: Determining the research plan, data analysis, All authors reviewed the manuscript.

Supplementary information

Increasing the acid–base alternating corrosion can effectively reduce:
1) the formation of inner wall island particles and further reduce the inner wall surface roughness. The particle peak height was reduced from 31.1 nm to 1.9 nm.
2) the dark current and the background noise.
3) Pointing to a new direction for improving the electrical properties of microchannel plates made of silicate glass.

Funding The project conducted in this research has not received any form of financial support or sponsor-ship. All research activities have been carried out by the researchers themselves, without any influence or control from any third-party organizations or individuals. We assure the objectivity and independence of the research findings, adhering to strict ethical standards and research guidelines.

Data Availability The data that support the findings of this study are available from the corresponding author upon reasonable request.

Declarations

This manuscript is an origin work and has not been published elsewhere in part or in entirety and is not under consideration by another journal. We have read and understood the journal's policies, and we believe that neither the manuscript nor the study violates any of these. There are no conflicts of interest to declare. We are looking forward to hearing your reply and with thanks for your kind consideration.

Ethical Approval The paper did not involve experiments related to human tissues and did not violate ethical and ethical requirements.

Consent for Publication All authors agreed to publish this research article.

Competing Interests The authors declare no competing interests.

References

1. Hans A, Schmidt P, Ozga C et al (2018) Extreme ultraviolet to visible dispersed single photon detection for highly sensitive sensing of fundamental processes in diverse samples[J]. Materials 11(6):869. https://doi.org/10.3390/ma11060869
2. Gys T (2015) Micro-channel plates and vacuum detectors[J]. Nucl Instrum Methods Phys Res, Sect A 787:254–260. https://doi.org/10.1016/j.nima.2014.12.044
3. Booth D, Rittenhouse ST, Yang J et al (2015) Production of trilobite Rydberg molecule dimers with kilo-Debye permanent electric dipole moments[J]. Science 348(6230):99–102. https://doi.org/10.1126/science.1260722
4. Priedhorsky W, Bloch J (2005) Optical detection of rapidly moving objects in space[J]. Appl Opt 44(3):423–433. https://doi.org/10.1364/AO.44.000423
5. Wiggins BB, deSouza ZO et al (2017) Achieving high spatial resolution using a microchannel plate detector with an economic and scalable approach - ScienceDirect[J]. Nucl Instrum Methods Phys Res A 872:144–149. https://doi.org/10.1016/j.nima.2017.08.032

6. Pertot Y, Schmidt C, Matthews M et al (2017) Time-resolved x-ray absorption spectroscopy with a water window high-harmonic source[J]. Science 355(6322):aah6114. https://doi.org/10.1126/science.aah6114
7. Barnyakov AY, Barnyakov MY, Prisekin VG et al (2017) Test of microchannel plates in magnetic fields up to 45 T[J]. Nucl Instrum Methods Phys Res 845(feb.11):588–590. https://doi.org/10.1016/j.nima.2016.05.131
8. Mazuritskiy MI, Dabagov SB, Lerer AM et al (2017) Transmission diffractive patterns of large microchannel plates at soft X-ray energies[J]. Nucl Instrum Methods Phys Res B 402(jul.1):282–286. https://doi.org/10.1016/j.nimb.2017.02.075
9. O'Mahony A, Craven CA, Minot MJ et al (2016) Atomic layer deposition of alternative glass microchannel plates[J]. J Vac Sci Technol A: Vac Surf Films 34(1):01A128. https://doi.org/10.1116/1.4936231
10. Ertley C, Siegmund O, Schwarz J et al (2015) Characterization of borosilicate microchannel plates functionalized by atomic layer deposition[C]. Conference on UV, x-ray, and gamma-ray space instrumentation for astronomy XIX. Experimental Astrophysics Group, Space Sciences Laboratory, 7 Gauss Way, University of California, Berkeley, CA 94720; Experimental Astrophysics Group, Space Sciences Laboratory, 7 Gauss Way, University of California, Berkeley, CA 94720; Experimental Astroph
11. Siegmund OHW, McPhate JB, Jelinsky SR et al (2013) Large area microchannel plate imaging event counting detectors with sub-nanosecond timing[J]. IEEE Trans Nuclear Sci 60(2):923–931. https://doi.org/10.1109/TNS.2013.2252364
12. Siegmund OHW, Gummin MA, Stock J et al (1993) Microchannel plate imaging detectors for the ultraviolet[J]. NTRS. https://doi.org/10.1117/12.283775
13. Rajopadhye NR, Bhoraskar SV, Chakravorty D (1988) Electron emissive properties of Pb and Bi containing glasses[J]. J Non-Cryst Solids 105(1–2):179–184. https://doi.org/10.1016/0022-3093(88)90354-7
14. Mizoshita S et al (1995) Secondary electron emission from solid surface in an oblique magnetic field[J]. J Nucl Mater 220(94):488–492. https://doi.org/10.1016/0022-3115(94)00509-5
15. Huang Y, Yang Z, Hui L et al (2011) XPS study on microporous surface composition of microchannel plates[J]. Proc SPIE Int Soc Opt Eng 8194(3):91–94. https://doi.org/10.1117/12.900283
16. Schultz-Münzenberg C, Meisel W, Gütlich P (1998) Changes of lead silicate glasses induced by leaching[J]. J Non Cryst Solids 238(1–2):83–90. https://doi.org/10.1016/S0022-3093(98)00580-8
17. Huang Y, Gu Z, Zhang Y et al (2012) Nano-scale morphology on micro-channel plate lead silicate glass surface[J]. Ku Suan Jen Hsueh Pao/ J Chin Ceram Soc 40(7):994–999
18. Pan S, Huang Y et al (2018) Composition diffusion of core and clad glass interface during thermal process of micro-channel plate. J Chin Ceram Soc 46(5):7. https://doi.org/10.14062/j.issn.0454-5648.2018.05.13
19. Ertley C, Siegmund OHW, Schwarz J, Mane AU, Minot MJ, Mahony AO, Craven CA, Popecki M (2015) Proc.SPIE 9601, 96010S